RSC Advances

ROYAL SOCIETY OF CHEMISTRY

www.rsc.org/advances

Chitosan Nanoparticle Carrier Based on Surface Molecularly Imprinted Polymers for the Recognition and Separation of Protein

Cenjin Zhang[a]， Yuzhi Wang[a]*, Junxia Guo[a],Yanjin Liu[a], Yigang Zhou [b]

[a] State Key Laboratory of Chemo/Biosensing and Chemometrics, College of Chemistry and Chemical Engineering, Hunan University, Changsha, 410082, P.R. China

[b] Department of Microbiology, College of Basic Medicine, Central South University, Changsha, 410083, P.R. China

Corresponding author: Professor Yuzhi Wang

State Key Laboratory of Chemo/Biosensing and Chemometrics

College of Chemistry and Chemical Engineering

Hunan University

Changsha 410082

P. R. China

Phone: +86-731-88821903

Fax: +86-731-88821848

E-mail: wyzss@hnu.edu .cn

Abbreviations: AA, acrylic acid; AAm, acrylamide; APS, ammonium persulfate; BSA, bovine serum albumin; BHb, bovine hemoglobin; CS, chitosan; FESEM, field emission scanning electron microscope; FT-IR, fourier transform infrared spectroscopy; GMA, glycidyl methacrylate;

GMA-CS, ethylene-modified chitosan; HAc, acetic acid; HCl, hydrochloric acid; Lyz, lysozyme; MBAA, N,N-methylene-bis-acrylamide; MIPs, molecularly imprinted polymers; NIP, non-imprinted polymer; OVA, ovalbumin; Qmax, theoretical maximum adsorption capacity; SDS, sodium dodecyl sulfate; SDS-PAGE, sodium dodecyl sulfate polyacrylamide gel electrophoresis; TEM, transmission electron microscope; TEMED, N,N,N`,N`-tetramethylenediamine; TG, thermogravimetric analysis; Tris, tris(hydroxymethyl)aminomethane

Abstract

This paper discussed the construction of surface molecularly imprinted polymers (MIPs) based on the modified chitosan (CS) nanoparticle carrier to recognize and separate bovine serum albumin (BSA, pI 4.9, MW 69.0 kDa) in aqueous solution. Functional biopolymer CS was selected as the supporting material. The C=C group was introduced to CS by glycidyl methacrylate (GMA) to form ethylene-modified chitosan (GMA-CS), so that the imprinting polymerization could be initiated onto GMA-CS. Both bi-functional monomers MIP1 composed of acrylamide (AAm) and acrylic acid (AA) and single functional monomer MIP2 polymerized only by AA were prepared. Transmission electron microscope (TEM) and field emission scanning electron microscope (FESEM) were used to characterize the micro-morphology of MIP1 and MIP2, respectively. Static adsorption experiments showed that the adsorption capacity of MIP2 for BSA was much higher than MIP1, so we chose MIP2 for further research. The results showed that the MIP2 could accomplish adsorption equilibrium within only 2 h under initial BSA concentration of 1.0 mg/mL and gave a imprint factor of 2.35. The theoretical maximum adsorption capacity (Q max) was determined by the Langmuir model, which turned out to be 373.13 mg/g. The selectivity of the MIP2 was evaluated by direct adsorption of a single reference protein and mixed proteins. The UV measurement and sodium dodecyl sulfate polyacrylamide gel electrophoresis (SDS-PAGE) analysis results indicated that the MIP2 had a relatively higher adsorption capacity with good recognition and binding selectivity for BSA, which made it possible to remove the template protein from different sample solutions. After three adsorption-desorption cycles, MIP2 still could maintain 66.5% of absorption capacity. It was also found that the pH of buffer had great influence on the adsorption capacity of MIP2, indicating electrostatic interactions played an important role in the absorption and recognition process.

Key Words: Surface Molecularly Imprinted Polymers / Chitosan Nanoparticle / Bovine serum albumin/ Recognition

1.Introduction

Molecule imprinting is a powerful method to prepare tailor-made synthetic polymers capable of molecular recognition by copolymerization of template molecule-functional monomer complexes and crosslinkers. After the removal of the template molecule from the resulting polymer network, specific binding cavities used as recognition sites for the template molecule are left which are composed of functional monomer residues assembled to fit the template molecule in terms of their size, shape, and exposed chemical functionality [1]. Because of its excellent advantages like specific recognition, high stability, low cost and reusability, MIP material can be applied in many fields of sensors [2-3], solid-phase extraction [4], separation [5-6],catalysis [7], water treatment [8] and drug design [9]. Despite the attractive features of MIP material, it has been largely limited to small molecules. The technique of protein imprinting to specifically recognize the target protein still remains a challenge, because proteins have their own characteristics of large molecular size, the high flexibility of spatial conformation, the complex surface structures [10]. The protein imprinted polymers can be used as cell scaffold material, antibodie and enzyme, which can substitute for natural biological structure [11-13]. Therefore, it is necessary to study deeply about the preparation of protein imprinted polymers.

However, due to the thick polymeric network, the MIPs prepared by the conventional bulky polymerization technique had some disadvantages especially for protein imprinting. For example, the polymeric network restricted the template molecule from removal and rebinding, which resulted in materials with poor site accessibility and low rebinding capacity for the target molecules [14-15]. Because the protein template molecules were easily entrapped in the matrices, the elution was difficult, the diffusion barrier for the template molecules was higher, the rate of mass

transfer was lower, and the template molecules were not easy to bind with recognition sites [16-17]. To overcome these drawbacks effectively and enhance the imprinted efficiency, the surface molecularly imprinted method in which imprinted polymerization system was formed on a support substrate material surface [18-19] even combined with nanotechnology[20-21] have been proposed in place of traditional bulky imprinting methods. For surface molecular imprinting, carbon nanotube [22], magnetic nanoparticles [23], silica particles [24] and quantum dots [25] have already been used as solid support materials.

CS is a kind of natural alkaline polysaccharose, which is a linear biopolymer consisting of β -(1,4)-2-acetamido - β -D -glucose units with excellent features like biodegradability, biocompatibility, nontoxicity, nonantigenicity, abundant source, hydrophilicity and low-cost nature [26]. It can set off a lot of chemical reactions which contains plenty of reactive hydroxyl and amino functional groups. So chitosan can be modified by acylation, alkylation, etherification, esterification, halogenation, etc. These controllable chemical modifications come out derivatives with different structures and chemical properties [27-31]. Owing to its advantage nature, chitosan and its derivatives have drawn wide attention in the biomedical field. Many researchers have made several attempts to apply the chitosan to the molecular imprinting technique. Wei [32] et al. have synthesized ametal ion imprinted chitosan resin, which could considerably enhance the adsorption capacity and selectivity of the metal ion. Guo [33] et al. have prepared hemoglobin protein molecularly imprinted polymers, using acrylamide as the functional monomer, and cross-linked chitosan beads as the supporting matrix. The obtained MIP showed a much higher adsorption capacity for hemoglobin than the NIP with the same chemical composition.

In this work, we attempted to employ the functional biopolymer CS as the supporting

substrate materials to improve the adsorption capacity of surface imprinting for the reason that CS had plenty of amino and hydroxyl groups might self-assemble onto the template protein by hydrogen bonding, hydrophobic interactions and van der Waals forces. The C=C group was introduced to CS from GMA so that imprinting polymerization could occur on the modified GMA-CS carrier, which could form the uniform and nano-sized production particles to offer high surface area for the adsorption of template. Both bi-functional monomers MIP1 composed of AAm with AA and single functional monomer MIP2 polymerized only by AA were prepared. After template protein BSA was removed by 10% (w/v) SDS-10% (v/v) acetic acid (HAc) eluent solution, specific binding sites that matched the template were obtained on MIPs. The resulting MIPs could effectively solve the problem of difficult elution, which was also conducive for the template protein rebinding process. MIP1 was characterized by TEM. MIP2 was characterized by FESEM, fourier transform infrared spectroscopy (FT-IR) and thermogravimetric analysis (TG). The recognition performance of MIP2 for BSA was further investigated by adsorption capacity, imprinting efficiency and specific selectivity through static adsorption tests.

2. Experimental sections

2.1 Instrumentation

A UV-2450 UV-vis spectrophotometer (Shimadzu, Japan) was used to determine the absorbance of protein. IR spectra were recorded on a FT-IR spectrometer (Perkin Elmer, USA). TG curves of samples were acquired by thermal gravimetric analyzer (Netzsch, Germany). Virtis freeze drier (YiKang Experimental Equipment Co. Ltd, China) was employed to get the freeze-dried polymers. After being dried, the samples were imaged under JEM-3010 transmission

electron microscopy (JEOL Company, Japan) or Hitachi S-4700 scanning electron microscope (Hitachi Company, Japan). QYC 200 incubator shaker (FuMa Experimental Equipment Co. Ltd, China) was used for static adsorption process. RM 220 ultrapure water instrument (LiDe Experimental Equipment Co. Ltd, China) was used throughout the experiments.

2.2 Chemicals and reagents

N,N-methylene-bis-acrylamide (MBAA), chitosan, glycidyl methacrylate was supplied by Aladdin chemistry Co., Ltd. (Shanghai, China). Acrylic acid, acetone, acetic acid, ammonium persulfate (APS), acrylamide, N,N,N`,N`-tetramethylenediamine (TEMED), hydrochloric acid (HCl), tris(hydroxymethyl)aminomethane (Tris), bovine serum albumin (BSA, MW 69kDa，pI 4.9), bovine hemoglobin (BHb, MW 65kDa, pI 6.9), ovalbumin (OVA, pI 4.7, MW 43.0kDa) were all purchased from Guoyao chemical reagents company Co., Ltd. (Beijing, China). Sodium dodecyl sulfate was purchased from FuCheng Chemical Reagent (Tianjin, China). Tris-HCl buffer solution (pH 7.0, 10 mM) was used as the working medium. All chemicals used were of analytical grade and used directly without further purification. Ultrapure water (18.25MΩ cm^{-1}) used throughout the experiment was obtained from the laboratory purification system.

2.3 Preparation of functional chitosan

Functional CS carrier were prepared by the introduction of C=C from GMA following a procedure reported by guan et al [34]. The synthesis process was shown in Fig. 1. In this experiment, 1 g of CS was resolved in 50 mL of 2% (v/v) HAc aqueous solution. The system was stirred for 1h at room temperature and deoxygenated by purging with nitrogen for 5 minutes, then 5.3 ml of GMA was added dropwise to the above aqueous solution of CS at the mole rate of vinyl: amino = 6:1. The reaction system was left to stand for 24 h at room temperature under nitrogen

atmosphere protection and magnetic stirring. After reaction, large amount of acetone was poured into the product solution to form functional CS precipitate. The precipitate was filtered and washed by acetone three times to remove unreacted GMA. Finally, the product was dried by virtis freeze drier to obtain ethylene-modified chitosan (GMA-CS).

2.4 Preparation of Imprinted and Non-imprinted Polymers

In this experiment, both bi-functional monomers MIP1 and single functional monomer MIP2 were prepared. Highly schematic representations of the preparation processes were shown in Fig. 2. At first, 100 mg of GMA-CS carrier was dispersed in 3 mL of Tris-HCl buffer solution (pH=7.0, 10 mM) with shaking for 30 minutes. Then, 40 mg of template protein BSA, 30 mg of crosslinkers MBAA, 90 mg of main functional monomer AAm combined with 60 uL of second functional monomer AA for MIP1 or 150 uL of single functional monomer AA for MIP2 were added into the GMA-CS solutions, with stirring for 2 h to obtain the completely self-assembled complexes on GMA-CS carriers. After the prepolymerization, the solutions were deoxygenated by purging with nitrogen for 8 minutes, then 40 ul of 20% wt initiator APS and 10 ul of TEMED were added. The reaction systems were purged with nitrogen for another 5 minutes and sealed immediately. The polymerization was carried out for 24 h at room temperature with shaking. Afterwards, the obtained polymers were first washed with solution of SDS(10%, w/v) and HAc(10%, v/v) to remove the template protein for several times until no BSA could be detected by a UV-vis spectrophotometer at 278 nm and then washed with ultrapure water to remove SDS. Finally, the imprinted polymers were obtained after drying by virtis freeze drier. The control non-imprinted polymers were also prepared and treated in the same way except for the addition of the template BSA.

2.5 Protein adsorption experiments

The adsorption performance of the MIPs were studied by adsorption experiments, including adsorption kinetics experiments, adsorption isothermal experiments, selectivity experiments and reusability experiments. The prepared hydrogels were first swollen in the Tris-HCl buffer (pH=7.0, 10 mM) to gain equilibrium prior to use. Adsorption experiments were conducted by incubating 5.0 mg of MIP or NIP in 4.0 mL of certain initial concentration protein Tris-HCl buffer solution (pH=7.0, 10 mM). All the adsorption experiments were conducted in the incubator shaker (200 r/min) under room temperature. After adsorption equilibrium, samples were centrifuged at 5000 rpm for 6 minutes. The concentration of protein in the supernatant was measured by detecting the absorbance at 278 nm for BSA and OVA and 404 nm for BHb using a UV-2450 UV-vis spectrophotometer. As an example, the UV-vis spectra of BSA was shown in Fig. 3. The capacity of protein adsorbed by the MIP or NIP was calculated by the following formula:

$$Q = \frac{(C_0 - C)V}{M} \quad (1)$$

Where Q was the mass of protein adsorbed onto one unit amount of polymer (mg /g), C_0 and C were the initial and equilibrium concentrations of protein solutions respectively (mg /mL), V was the initial volume of the protein solution (mL), and M was the mass of polymer (g).

The specific recognition characteristic of the MIP was evaluated by the imprinting factor α which was defined by following formula:

$$\alpha = Q_{MIP}/Q_{NIP} \quad (2)$$

Where Q_{MIP} and Q_{NIP} were adsorption capacities of MIP and NIP for a tested protein, respectively.

In the adsorption kinetics experiments, the initial concentration of BSA was 1.0 mg/mL. The concentration of BSA at different time was measured using a UV-vis spectrophotometer at a wavelength of 278 nm. Adsorption isothermal experiments were performed by adsorption of a series of different initial concentration of BSA solutions (0.2 – 1.6 mg/mL) for 2 h.

In the selectivity experiments, BHb (1.0 mg/mL) and OVA (1.0 mg/mL) were chosen as the reference proteins to prove the selectivity of MIP towards the template protein BSA (1.0 mg/mL). The concentration of each protein was measured by the UV-vis spectrophotometer at their own maximum absorption wavelength. For the mixed adsorption experiments, OVA was chosen as the competitive protein. The adsorption was performed with a protein mixture (containing 1.0 mg/mL of OVA and 1.0 mg/mL of BSA). 10 uL of the mixed solution, before and after the adsorption, was extracted for SDS-PAGE analysis with a 12% polyacrylamide separation gel. In the reusability experiment, the MIP was subjected to 3 times adsorption-desorption cyclic operation. SDS-HAc was used as elution for complete removal of BSA adsorbed on MIP to free the imprinted sites and make MIP regain the ability to adsorb protein.

In adsorption experiments, the adsorption capacity of MIP1 and MIP2 for BSA at initial protein concentration of 1.0 mg/mL after adsorption time of 7 h were compared. The result showed that the adsorption capacity of MIP2 was 369.93 mg/g, which was much higher than that of MIP1 whose adsorption capacity value was 50.25 mg/g. The difference of adsorption capacity between MIP1 and MIP2 might be related to the thickness of the polymer layer. In the synthetic process of MIP2, 150 uL of AA was used as functional monomer. While in MIP1, 90 mg of AAm and 60 uL of AA was used as bi-functional monomer, which could increase the thickness of the polymer layer. And then blocked the site accessibility and led to the decrease in the binding

amount of BSA. So we selected MIP2 and NIP2 for all the subsequent experiments.

2.6 Characterization of polymers

The surface morphologies of GMA-CS, MIP2 and NIP2 were determined by SEM. TEM was mainly used to confirm nano-sized GMA-CS carrier particle, besides, MIP1 and NIP1 were also characterized by TEM. The CS, GMA-CS, MIP2 and NIP2 were characterized by an FT-IR spectrometer in the range of 4000-500 cm^{-1} to verify the successful synthesis of the MIP2 on the surface of GMA-CS carrier. TG curves of GMA-CS, MIP2 and NIP2 were acquired to further verify the relative composition of the prepared materials.

3. Results and discussion

3.1 Characterizations of the prepared materials

SEM images of GMA-CS (a), MIP2 (b) and NIP2 (c) were shown in Fig. 4 to characterize their surface morphology and microstructure. As seen from the images, the surface morphology of the prepared materials were different from each other. The surface of GMA-CS carrier was very smooth with compact and dense microstructure. After grafting with AA, MIP2 and NIP2 with extra polymer layer appeared rough surface morphology in SEM images. In addition, when carefully compared MIP2 with NIP2, it can be found that although the porosity couldn't be obviously seen on the surface of MIP2, the MIP2 had a relatively rougher surface, indicating the success of the polymerization in the presence of the temple protein.

TEM images of GMA-CS (d), NIP1 (e) and MIP1 (f) were shown in Fig. 4 to characterize their microscopic size and shape. Uniform and regular spherical particle structure could be observed from all of the three TEM images, which verified the successful formation of desired material shape. It could be clearly observed that the average diameters of GMA-CS, NIP1 and MIP1 were different

from each other. Compared with the GMA-CS whose diameter was ranging from 30 to 40 nm, the prepared NIP1 and MIP1 had a much bigger size with diameter ranging from 110 to 120 nm and 150 to 160 nm, respectively. This meant the modified polymer layer were successfully grafted onto the surface of GMA-CS carrier during polymerization. After the preparation of MIP1 and NIP1 were successfully proved by TEM images, and the much higher absorption capacity of MIP2 for BSA when compared with MIP1, we only selected MIP2 and NIP2 for the further characterization.

In order to further determine the chemical structure of the synthetic products, FT-IR spectras of GMA-CS (a), CS (b), NIP2 (c) and MIP2 (d) were shown in Fig. 5A. As could be seen from the figure, compared with CS, GMA-CS showed a new peak at 1637 cm^{-1} which could be ascribed to C=C. In our work, C=C was successfully introduced to CS by GMA. The FT-IR spectras of NIP and MIP were similar to each other in terms of pattern profile, and they both had some new peaks when compared with GMA-CS. The new characteristic peak of 1728 cm^{-1} and other two observed new peaks 3430 cm^{-1} and 3150 cm^{-1} could be ascribed to the C=O and of O−H bond in -COOH group from AA. This FT-IR spectrum verified that the functional monomer have been successfully grafted onto the surface of GMA-CS after imprinting polymerization.

Thermogravimetric analysis was performed to further explore the thermal stability and structure characteristic of the prepared products. TG curves of (a) NIP2, (b) MIP2 and (c) GMA-CS were shown in Fig. 5B. From the figure, we could find that the TG curves of NIP2, MIP2 and GMA-CS were quite different from each other with the temperature changing from 0℃ to 800℃. When the temperature reached 800℃, the weight of GMA-CS, NIP2 and MIP2 were lost to 36%, 25% and 17% of their initial weight, respectively. This illustrated that the thermal stability of polyacrylic acid outer layer was weaker than the carrier material GMA-CS which was also a kind of polymer. But in

the temperature range from 100℃ to 200℃, the degree of weight lost ranked by GMA-CS > MIP2 > NIP2. Considering the weight loss of the above temperature range was mainly caused by water evaporation, we could speculate that GMA-CS carrier was a kind of material with great water adsorption capacity and the water adsorption capacity of MIP2 and NIP2 decreased when a layer of polyacrylic acid was modified on the surface of GMA-CS carrier. Besides, the greater water adsorption capacity of MIP2 than NIP2 might be explained by the existing of imprinted cavity on MIP2.

3.2 Swelling measurement

As an important feature of hydrogels material, the saturated swelling ratio was investigated in swelling studies. The saturated swelling ratio(S) was calculated from the following equation:

$$S = \frac{W - W_0}{W_0} \quad (3)$$

Where W is the mass of the swollen gel, and W_0 is the mass of the dry gel.

In our study, the results of the saturated swelling ratio of GMA-CS, MIP2 and NIP2 were shown in Table 1. It can be seen that the saturated swelling ratio of MIP and NIP corresponded to 3.66 and 3.14, which was much lower than that of GMA-CS (13.79). This was because there were plenty of hydrophilic amino and carboxyl functional groups on the surface of CS, which could adsorb a lot of water. However, the diffusion and penetration resistance of water molecules would increase when the CS was coated with polymer, which could decrease the water absorbency of hydrogels material. Therefore, the results proved the successful grafting of PAA on the surface of GMA-CS.

3.3 Adsorption Kinetics

In the evaluation for adsorption kinetics, the adsorption capacities of the MIP2 and NIP2 were

tested as a function of time. The kinetics curves were shown in Fig.6a. From the figure, we could see that the adsorption capacities of both MIP2 and NIP2 for BSA increased as time goes by and they could adsorb template protein quickly and easily owing to the low mass transfer resistance of thin shell. The adsorption equilibrium time for MIP2 and NIP2 were 2 h and 4 h, respectively. In addition, MIP2 obviously adsorbed more template protein compared to NIP2 under the same conditions. This result also validate the ability of MIP2 to recognize the template and confirmed the fact that recognition sites with the specific shape and the orientation of functional groups were successfully formed in the imprinted polymer network during the imprinting process. The relatively higher adsorption capacity of MIP2 compared with NIP2 could be attributed to the electrostatic interaction and hydrogen bonding interaction between -COOH group of MIP2 and template protein BSA. However, the NIP had no recognition sites for BSA, the adsorption capacity was mainly from non-specific adsorption.

3.4 Adsorption Isotherms

To investigate the adsorption capacities of both MIP2 and NIP2 for BSA, the adsorption isotherms were tested under room temperature with different initial concentration of BSA solutions and the results could be seen in Fig. 6b. As the isotherm curves showed, the adsorption trend of NIP2 was similar to MIP2. They both rose with the increase of the initial BSA concentration from 0.2 mg/mL to 1.0 mg/mL. Then these curves became flat and reached thermodynamic equilibrium in the concentration region above 1.0 mg/mL. So the concentration of 1.0 mg/mL was chosen as the optimal concentration condition for the following experiments. It also can be found that the adsorption capacities of MIP2 and NIP2 were almost the same in the low concentration region of 0.2 mg/mL to 0.4 mg/mL, which indicated that the existing of serious non-specific adsorption and the

limited amount of proteins were completely absorbed by non-specific adsorption before imprinted sites were used. MIP2 showed much higher adsorption capacity than NIP2 when the BSA initial concentration increased to 0.6 mg/mL or more, and good imprinting imprinting effect could be obtained with a imprinting factor α of 2.35 at the BSA initial concentration of 1.0 mg/mL, which also suggested that the specific recognition sites were successfully formed on MIP2 by the imprinting template molecule BSA during the polymerization process.

The adsorption thermodynamic experiment datas of MIP2 could be further analyzed according to Langmuir isotherm model which was proposed by Irving Langmuir [35]. The equation of Langmuir model was listed as following:

$$C_e/Q=C_e/Q_{max}+1/(KQ_{max}) \quad (4)$$

Where C_e was the adsorption equilibrium concentration of BSA, Q was the adsorption capacity of MIP2 at equilibrium concentration, Q_{max} was the theoretical maximum adsorption capacity of MIP2, and K was the Langmuir adsorption equilibrium constant.

A highly linearized plot of C_e /Q versus C_e was presented in Fig. 6c. It could be seen that the Langmuir equation fitted well for the adsorption of BSA on MIP2 within the concentration range studied (correlation coefficient, $r^2 = 0.99902$). The value of Q_{max} was equal to the reciprocal of the slope of Langmuir equation simulated linear curve, which turned out to be 373.13 mg/g. This result evidenced a relatively high adsorption affinity for our synthesized MIP2 towards BSA.

3.5 Selectivity adsorption

In order to study the selectivity of MIP2 towards BSA, reference proteins BHb and OVA were used in selective adsorption experiment. This choice was based on the fact that BHb had the same molecular weight and OVA had the same isoelectric point as template BSA. The adsorption

capacities of MIP2 and NIP2 for these three proteins were illustrated in Fig. 7a. It could be seen from the figure that, MIP2 obviously displayed a higher adsorption capacity for template BSA than the other two reference proteins, indicating the high adsorption selectivity of MIP2 for BSA. Moreover, a comparison of the adsorption of the MIP2 and NIP2 for each protein substrate suggested that MIP2 had no imprinting effect for BHb and OVA because both MIP2 and NIP2 nearly had the same adsorption capacity for them.

The selectivity factor β was used to evaluate the specific selectivity and was defined by following formula:

$$\beta = \alpha_{BSA}/\alpha_{RP} \quad (5)$$

Where α_{BSA} and α_{RP} were tested imprinting factor for template protein BSA and particular reference protein. The values of imprinting factor α and selectivity factor β for BSA, BHb, and OVA were calculated and listed in Table 2. It was observed that α value of MIP2 for BSA was much higher than those for BHb and OVA, which meant that MIP2 had pronounced adsorption selectivity for template BSA when compared with other two reference proteins. In addition, the β values for BHb and OVA were around 2.0, which again indicated the MIP2 had higher adsorption selectivity than that of the NIP2.

The selectivity of MIP2 for BSA in mixture of proteins was also studied. In this test, OVA was selected as the competitive protein. The result of SDS-PAGE analysis was shown in Fig. S1. From the degree of change in the band width and color of gel electrophoresis, we could find that BSA was the most adsorbed protein by MIP2. Although both BSA and OVA were adsorbed by the NIP2, but the adsorption capacities were much lower than those of MIP2. So good selectivity was observed.

The preferred adsorption and selective recognition of MIP2 for template BSA might be due to

the presence of imprinted recognition sites formed during imprinting process, which only matched with template BSA in shape, size and arrangement of functional groups. However, the different spatial structure of reference proteins did not match the imprinted sites and their access to the imprinted binding cavities might be limited by the steric hindrance of polymer chains. Thus the adsorption capacity of MIP2 for reference proteins were relatively lower than that for BSA, and mainly came from physical adsorption associated with nonspecific interactions. As for NIP2, the nonspecific adsorption was the dominant driving force because of lacking imprinted recognition sites. Therefore, the adsorption capacity of NIP2 for BSA was much lower than MIP2.

3.6 Regeneration feature

In order to investigate the reuse property, MIP2 was regenerated by eluent of SDS(10%, w/v) and HAc(10%, v/v) after BSA adsorption process. In this work, MIP2 was repeatedly used for three times, and the adsorption capacity of MIP2 for each adsorption experiment was measured and shown in Fig. 7b. After once time adsorption-desorption cycle, the adsorption capacity of MIP2 for BSA was about 82.93% relative to that in the first adsorption experiment, and maintained at 66.45% in the third adsorption experiment. The lost adsorption capacity of MIP2 after repeat adsorption might be due to the damage of some imprinted binding sites for BSA in the template removal operation progress. Although ideal reuse efficiency of MIP2 was not achieved in this study, but MIP2 still maintained a certain degree of capacity adsorption for BSA, indicating the imprinted cavities could regain the ability to adsorb template protein BSA and MIP2 could be used repeatedly for several times.

3.7 Effect of buffer pH on the adsorption of BSA

In order to study the mechanism for static adsorption of BSA onto MIP2 and verify the

399 important role electrostatic interaction played during adsorption process, a series of Tris-HCl buffer
400 solutions with different pH values were prepared as the working medium to test the effect of buffer
401 pH on the adsorption capacity of MIP2 and NIP2 for BSA. The different pH values of Tris-HCl
402 buffer could change the nature and the amount of electric charge on the protein, leading to various
403 nature and extent of electrostatic interactions between the protein and imprinted cavities on MIP2
404 during adsorption. If the electrostatic interaction was the main driving force in adsorption process,
405 the adsorption capacity of MIP2 or NIP2 for BSA under different pH environment would be
406 significantly different from each other. The result presented in Table 3 was the case. This might be
407 due to the functional monomer acrylic acid could ionize and form negatively charged carboxylate
408 ions $-COO^-$ on the polymer side chain in aqueous solution after polymerization, which could interact
409 with the different parts of the protein by electrostatic interactions.
410 When the pH of the buffer was bigger than 8.5, the BSA protein molecule carried a lot of
411 negative charge and formed strong electrostatic repulsion interaction with $-COO^-$ in MIP2, leading to
412 zero adsorption capacity of MIP2 for BSA. However, the adsorption capacity of MIP2 for BSA at
413 buffer pH value of 7 was higher than that at buffer pH value of 6. This might be because 7 was also
414 the pH value chosen in imprinting polymerization process, the conformation of adsorption substrate
415 BSA have similar charge distribution and morphology as imprinted template BSA could better match
416 the imprinted cavity when the pH value in the adsorption process was the same as the pH value in
417 the imprinting polymerization process. The maximum adsorption capacity of MIP2 appeared at the
418 buffer pH value of 4. Taking into account the BSA isoelectric point of 4.9, the BSA should carry
419 some positive charge at buffer pH value of 4 and could form electrostatic attraction interaction with
420 $-COO^-$ in MIP2, which could greatly improve the affinity between BSA and MIP2. When the pH

421 value of the buffer further reduced to 2, the adsorption capacity of MIP2 for BSA was relatively low
422 within the whole test pH range. It might be because too low pH value of the environment would
423 inhibit the ionization of -COOH in MIP2 and reduce electrostatic attraction interaction between BSA
424 and MIP2. Moreover, there were large number of hydrogen ions H^+ in buffer at pH value of 2, which
425 would compete with BSA for the electrostatic interaction sites in MIP2 and further reduce the
426 affinity between BSA and MIP2, resulting in low adsorption for MIP2 towards BSA. Meanwhile,
427 NIP2 behaved similarly to MIP2 in the same series of buffer, which further validated the above
428 speculation and interpretation. Because both the imprinted cavities of MIP2 and polymer shell of
429 NIP2 were fulled with a lot of ionizable carboxyl groups which had a great tendency to form
430 electrostatic interaction.

431 Although MIP2 had the highest adsorption capacity at the buffer pH value of 4, considering the
432 protein was unstable and easy to lose the biological activity in acidic medium, so we still chose the
433 buffer with pH value of 7 as the working medium in the batch adsorption experiments.

434 **4. Conclusions**

435 In our work, a new kind of surface molecular imprinted polymer was successfully synthesized
436 to recognize the template protein BSA based on supporting material GMA-CS carrier. AA was used
437 as functional monomer and MBAA was adopted as cross-linker. The C=C group was introduced to
438 CS by GMA to facilitate imprinting polymerization. The results of the batch adsorption experiments
439 demonstrated that MIP2 could successfully recognize BSA. MIP2 had much higher adsorption
440 capacity for BSA when the testing concentration was above 0.6 mg/mL and offered faster adsorption
441 kinetic rate than NIP2. The equilibrium adsorption isotherms of BSA on MIP2 could be well fitted
442 by the Langmuir adsorption model and gave a theoretical maximum adsorption capacity of 373.13

mg/g. At the same time, the selectivity of the MIP2 for BSA was verified by direct adsorption of single reference protein and competitive adsorption of mixed protein. The results of all the experiments suggested that specific imprinted recognition sites which were complementary to BSA were created during the imprinting polymerization step. In addition, MIP2 could be reused after three adsorption-desorption cycles with reuse efficiency of 66.45%. Effect of buffer pH on the adsorption of BSA was also determined, and the result indicated that electrostatic interaction between BSA and MIP2 was the main driving force in adsorption. All the above mentioned advantageous features such as easy preparation, fast mass transfer rate, satisfied adsorption capacity and specific recognition capability to the template protein BSA proved that this method and MIP2 material provide a promising potential for the practical application in the field of protein rapid separation and enrichment for the near future.

Acknowledgements

The authors greatly appreciate the financial supports by the National Natural Science Foundation of China (No. 21175040; No. 21375035; No.J1210040) and the Foundation for Innovative Research Groups of NSFC (Grant 21221003).

References

1 N. Masque´, R. M. Marce´, F. Borrull, P. A. G. Cormack and D. C. Sherrington, *Anal. Chem.*, 2000, **72,** 4122-4126.

2 J. Niu, Z. H. Liu, L. Fu, F. Shi, H. W. Ma, Y. Ozaki and X. Zhang, *Langmuir,* 2008, **24**, 11988-11994.

3 J. W. Zhang, Y. L. Liu, G. L. Wu, M. Schönhoff and X. Zhang, *Langmuir,* 2011, **27**,

10370-10375.

4 F. Augusto, E. Carasek, R. G. Silva, S. R. Rivellino, A. D. Batista and E. Martendal, *J. Chromatogr. A*, 2010, **1217**, 2533-2542.

5 J. P. Wang, A. G. Cormack, D. C. Sherrington and E. Khoshdel, *Angew. Chem., Int. Ed. Engl.*,2003, **42**, 5336-5338.

6 H. Kubo, T. N. Player, S. Shinoda, H. Tsukube, H. Nariai and T. Takeuchi, *Anal. Chim.Acta*, 2004, **504**, 137-140.

7 C. D. Anderson, K. J. Shea and S. D. Rychnovsky, *Org.Lett.*, 2005, **7**, 4879-4882.

8 T. Kobayashi, P. S. Reddy, M. Ohta, M. Abe and N. Fujii, *Chem. Mater.,* 2002, **14**, 2499-2505.

9 C. J. Allender, C. Richardson, B. Woodhouse, C. M. Heard and K. R. Brain, *Int. J. Pharm.*, 2000, **195**, 39-43.

10 C. Alexander, H. S. Andersson, L. I. Andersson, R. J. Ansell, N. Kirsch, I. A. Nicholls, J. O'Mahony and M. J. Whitcombe, *J. Mol. Recognit.*, 2006, **19**, 106-180.

11 S. M. Reddy, Q. T. Phan and H. El-Sharif, *Biomacromolecules*, 2012, **13**, 3959-3965.

12 E.L. Holthoff and F.V. Bright, *Anal. Chim. Acta*, 2007, **594**, 147-161.

13 J. Gao, H. Tian and Y. Wang, *Biomaterials*, 2012, **33**, 3344-3352.

14 Y. Jin, M. Jiang, Y. Shi, Y. Lin, K. Peng and B. Dai, *Anal. Chim. Acta*, 2008, **612**, 105-113.

15 Q. Z. Feng, L. X. Zhao, W. Yan, J. M. Lin and Z. X. Zheng, *J. Hazard. Mater.*, 2009, **167**, 282-288.

16 C. Y. Huang, M. J. Syu, Y. S. Chang, C. H. Chang, T. C. Chou and B. D. Liu, *Biosens. Bioelectron.*, 2007, **22**, 1694-1699.

17 J. L. Urraca, M. C. Moreno-Bondi, G. Orellana, B. Sellergren and A. Hall, *J. Anal. Chem.*, 2007, **79**, 4915-4923.

18 T. Shiomi, M. Matsui, F. Mizukami and K. Sakaguchi, *Biomaterials*, 2005, **26**, 5564-5571.

19 X. P. Jia, M. L. Xu and Y. Z. Wang, *Analyst*, 2013, **138**, 651-658.

20 C. J. Tan and Y. W. Tong, *Langmuir*, 2007, **23**, 2722-2730.

21 C. J. Tan, S. Wangrangsimakul and R. Bai, *Chem. Mater.*, 2008, **20**, 118-127.

22 R. Liu, M. Sha, S. S. Jiang, J. Luo and X. Y. Liu, *Talanta*, 2014, **120**, 76-83.

23 Q. Q. Gai, F. Qu, Z. J. Liu, R. J. Dai and Y. K. Zhang, *J. Chromatogr., A*, 2010, **1217**, 5035-5042

24 W. Cheng, Z. Liu and Y. Wang, *Talanta*, 2013, **116**, 396-402.

25 W. Zhang, X. W. He, Y. Chen, W. Y. Li and Y. K. Zhang, *Biosens. Bioelectron.*, 2011, **26**, 2553-2558

26 F. L. Mi, Y. C. Tan, H. F. Liang and H. W. Sung, *Biomaterials*, 2002, **23**, 181-191.

27 Z. Y. Wang, Z. J. Jiang and X. Q. Hu, *Chinese Journal of Applied Chemistry,* 2002, **19**, 1002-1004.

28 F. Li, *Chemical Industry and Engineering,* 2002, **19**, 281-285.

29 H. Y. Hao, *Polymer Materials Science and Engineering,* 2006, **22**, 223-226.

30 A. B. Huang, *New Chemical Materials,* 2010, **38**, 17-20.

31 D. H.Li, *Chinese Journal of Biochemical Pharmaceutics,* 2002, **23**, 124-126.

510 32 T. T. Wei, H. X. Jing and D. W. Xia, *J. Chem. Technol. Biotechnol.*, 2001, **76**,
511 191-195.
512 33 T. Y. Guo, Y. Q. Xia and G. J. Hao, *Carbohydr. Polym.*, 2005, **62**, 214-221.
513 34 H. M. Guan and Y. J. Tong, *Sci. Tech. Engng*, 2009, **9**, 2038-2041.
514 35 I. Langmuir, *J. Am. Chem. Soc.*, 1916, **38**, 2221-2295.
515
516

517 **Table 1 Saturated swelling ratio of three samples**

Samples	GMA-CS	MIP2	NIP2
Saturated swelling ratio	13.79	3.66	3.14

518 **Table 2 Values of imprinting factor α and selectivity factor β for BSA, BHb and OVA.**

Protein	Q_{MIP} (mg/g)	Q_{NIP} (mg/g)	Imprinting factor α	Selectivity factor β
BSA	384.59	163.96	2.35	--
BHb	155.94	153.42	1.02	2.30
OVA	231.31	187.75	1.23	1.91

519
520

521 **Table 3** Effect of buffer pH on the adsorption capacity of MIP2 for BSA**.**

522

Buffer pH	2	4	6	7	8.5	10
Q_{MIP} mg/g	276.04	437.18	301.63	384.59	0	0
Q_{NIP} mg/g	58.57	231.63	152.08	163.96	0	0
mprinting factor α	4.71	1.89	1.98	2.35	0	0

523

524

525 **Figure captions**

526 Figure 1 Reaction diagram of GMA-Chitson.

527 Figure 2 Schematic representation of the molecular imprinting procedures for MIP1 and MIP2.

528 Figure 3 UV–vis spectrum of BSA in pure water.

529 Figure 4 SEM images of GMA-CS (a), MIP2 (b), NIP2(c) and TEM images of GMA-CS (d),

530 NIP1 (e) and MIP1(f).

531 Figure 5 (A) FT-IR spectra of GMA-CS (a), CS (b), NIP2 (c) and MIP2 (d), and (B) TG curves of

532 (a) NIP2, (b) MIP2 and (c) GMA-CS.

533 Figure 6 (a) Adsorption kinetics curves of the BSA on MIP2 and NIP2, (b) Adsorption isotherms

534 of the BSA on MIP2 and NIP2, and (c) Langmuir adsorption thermodynamics model of

535 MIP2 for curve of Ce / Q versus Ce.

536 Figure 7 (a) Selective adsorption between reference proteins and BSA on MIP2 and NIP2, and (b)

537 Influence of adsorption times on BSA adsorption capacity to the MIP2.

538

539

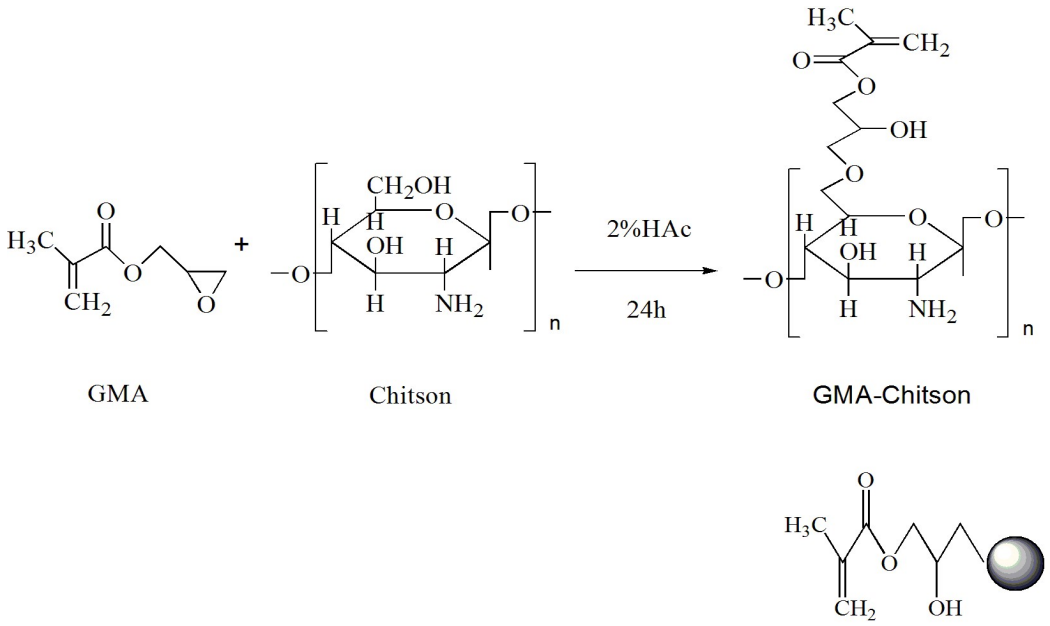

GMA-Chitson

Figure 1 Reaction diagram of GMA-Chitson.

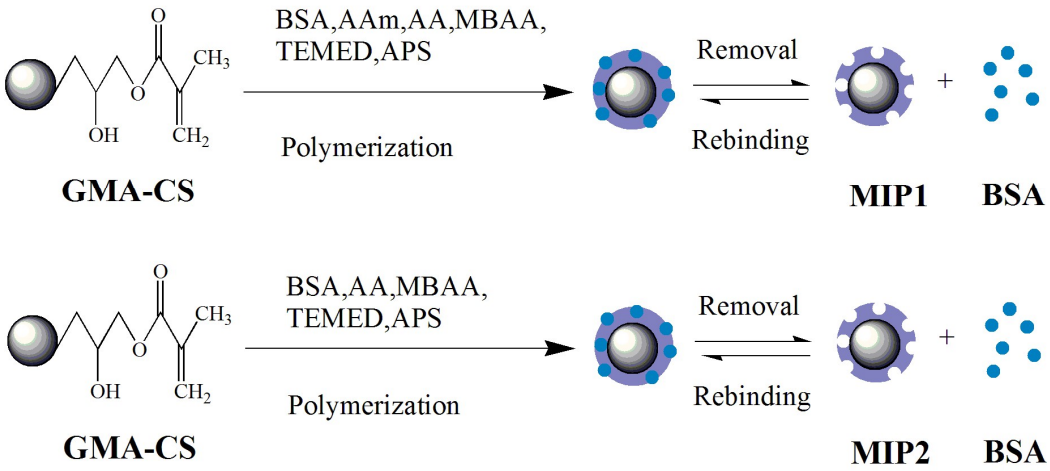

543

544 Figure 2 Schematic representation of the molecular imprinting procedures for MIP1 and MIP

545

546

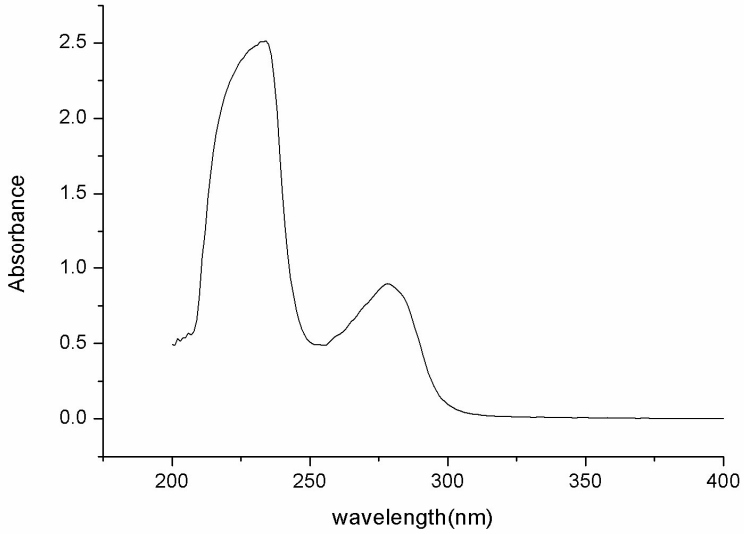

547

548 Figure 3 UV–vis spectrum of BSA in pure water.

549

550

551

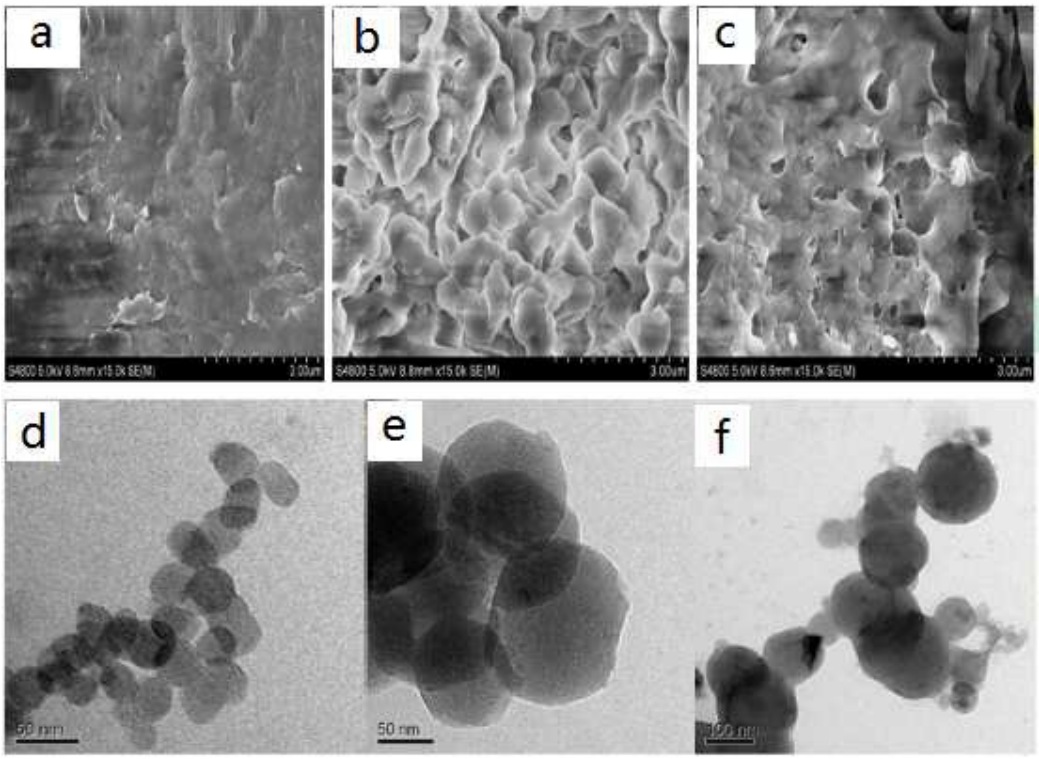

552

553 Figure 4 SEM images of GMA-CS (a), MIP2 (b), NIP2(c) and TEM images of GMA-CS (d),

554 NIP1 (e) and MIP1(f).

555

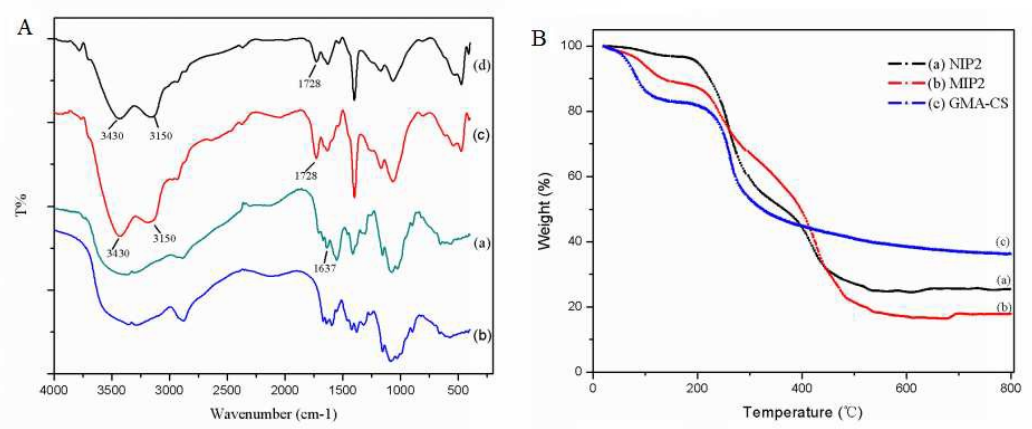

556

557 Figure 5 (A) FT-IR spectra of GMA-CS (a), CS (b), NIP2 (c) and MIP2 (d), and (B) TG curves of

558 (a) NIP2, (b) MIP2 and (c) GMA-CS.

559

560

561 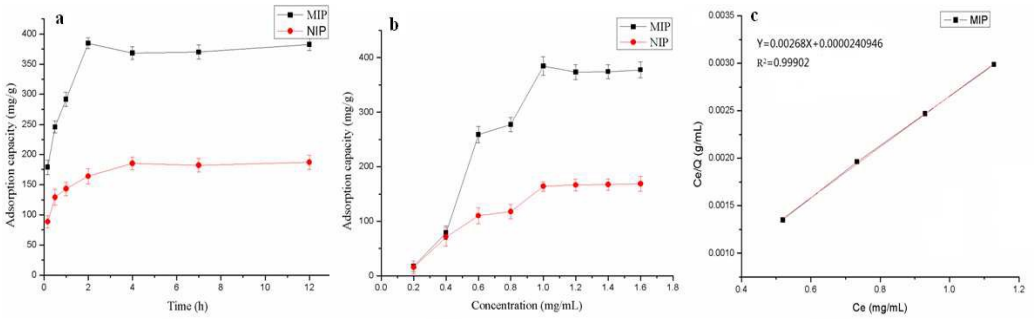

562 Figure 6 (a) Adsorption kinetics curves of the BSA on MIP2 and NIP2, (b) Adsorption isotherms
563 of the BSA on MIP2 and NIP2, and (c) Langmuir adsorption thermodynamics model of MIP2 for
564 curve of Ce / Q versus Ce.

565

566

567

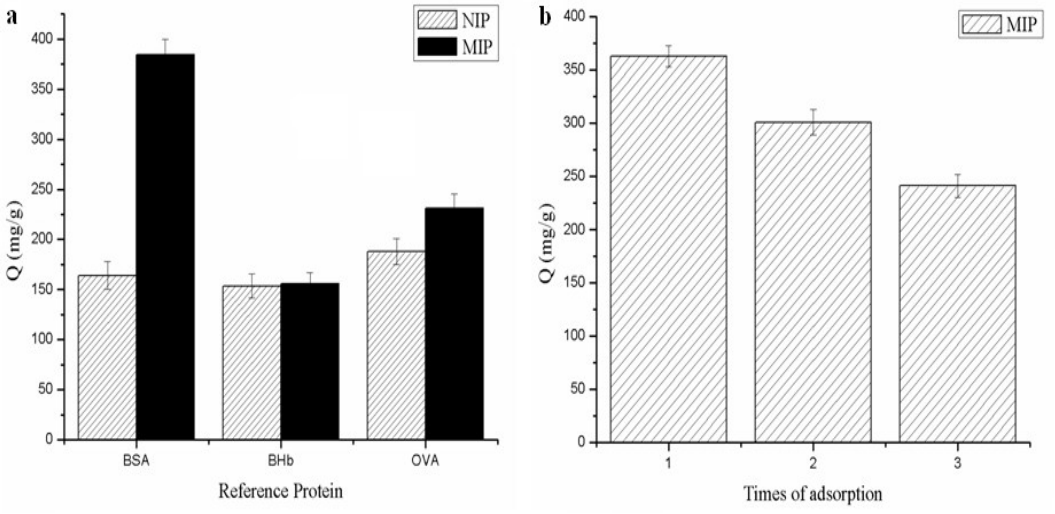

568 Figure 7 (a) Selective adsorption between reference proteins and BSA on MIP2 and NIP2, and (b)

569 Influence of adsorption times on BSA adsorption capacity to the MIP2.